Relay ARQ Strategies for Single Carrier MIMO Broadband Amplify-and-Forward Cooperative Transmission

Zakaria El-Moutaouakkil
Nokia Siemens Networks, Morocco

This work is co-authored with
Tarik Ait-Idir (INPT, Morocco/Telecom Bretagne, France)
Halim Yanikomeroglu (Carleton University, Canada)
Samir Saoudi (Telecom Bretagne, France)

IEEE Symposium on Personal Indoor and Mobile Radio Communications

29th September 2010

Outline

Brief Description of the Concept

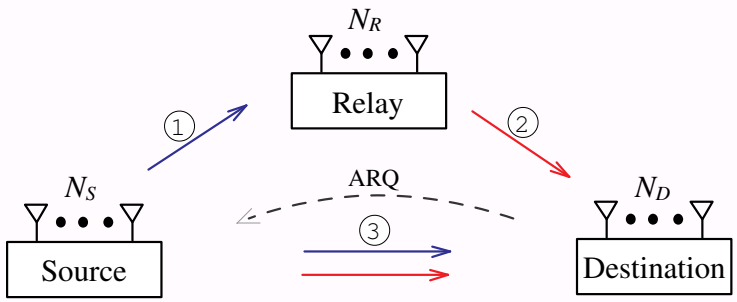

Fig. 1: Relay ARQ System Model

- Channel 1, channel 2, and channel 3 are regarded at kth transmission as a frequency selective fading MIMO channels having L_{SR}, L_{RD}, and L_{SD} independent paths, respectively.
- Each path is characterized by its quasi-static flat fading MIMO channel matrix $\mathbf{H}_l^{AB(k)} \in \mathbb{C}^{N_A \times N_B}$ for $l \in \{0, \ldots, L_{AB} - 1\}$ where $A \in \{S, R\}$ and $B \in \{R, D\}$.
- Relaying works under the framework of half-duplex amplify-and-forward protocol.
- Packet re-transmissions follows the Chase-type ARQ mechanism.
- Each Packet transmission k within a maximum of K ARQ rounds spans two consecutive time slots (TS)s.

Brief Description of the Concept

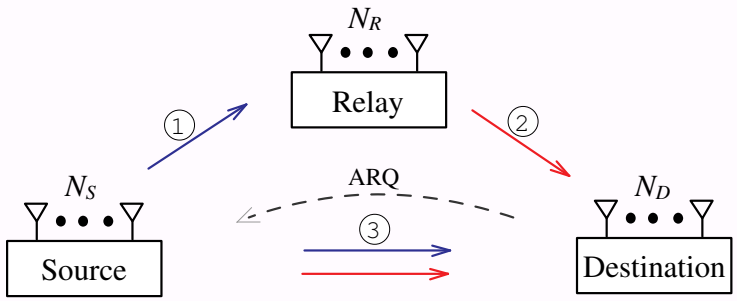

Fig. 1: Relay ARQ System Model

- Channel 1, channel 2, and channel 3 are regarded at kth transmission as a frequency selective fading MIMO channels having L_{SR}, L_{RD}, and L_{SD} independent paths, respectively.
- Each path is characterized by its quasi-static flat fading MIMO channel matrix $\mathbf{H}_l^{AB(k)} \in \mathbb{C}^{N_A \times N_B}$ for $l \in \{0, \ldots, L_{AB} - 1\}$ where $A \in \{S, R\}$ and $B \in \{R, D\}$.
- Relaying works under the framework of half-duplex amplify-and-forward protocol.
- Packet re-transmissions follows the Chase-type ARQ mechanism.
- Each Packet transmission k within a maximum of K ARQ rounds spans two consecutive time slots (TS)s.

Brief Description of the Concept

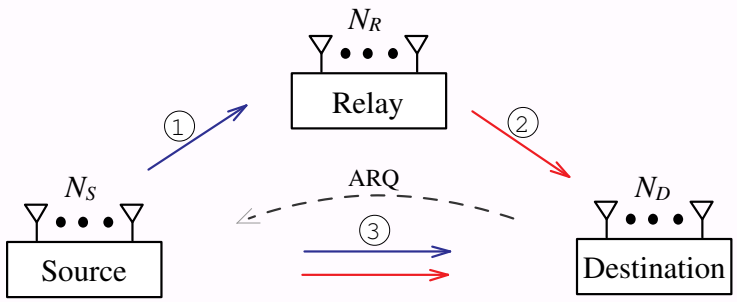

Fig. 1: Relay ARQ System Model

- Channel 1, channel 2, and channel 3 are regarded at kth transmission as a frequency selective fading MIMO channels having L_{SR}, L_{RD}, and L_{SD} independent paths, respectively.
- Each path is characterized by its quasi-static flat fading MIMO channel matrix $\mathbf{H}_l^{AB(k)} \in \mathbb{C}^{N_A \times N_B}$ for $l \in \{0, \ldots, L_{AB} - 1\}$ where $A \in \{S, R\}$ and $B \in \{R, D\}$.
- Relaying works under the framework of half-duplex amplify-and-forward protocol.
- Packet re-transmissions follows the Chase-type ARQ mechanism.
- Each Packet transmission k within a maximum of K ARQ rounds spans two consecutive time slots (TS)s.

Brief Description of the Concept

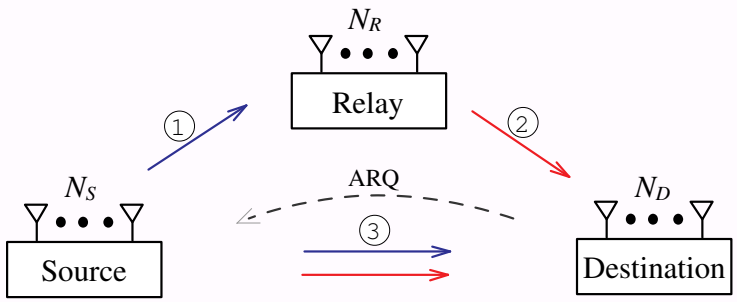

Fig. 1: Relay ARQ System Model

- Channel 1, channel 2, and channel 3 are regarded at kth transmission as a frequency selective fading MIMO channels having L_{SR}, L_{RD}, and L_{SD} independent paths, respectively.
- Each path is characterized by its quasi-static flat fading MIMO channel matrix $\mathbf{H}_l^{AB(k)} \in \mathbb{C}^{N_A \times N_B}$ for $l \in \{0, \ldots, L_{AB} - 1\}$ where $A \in \{S, R\}$ and $B \in \{R, D\}$.
- Relaying works under the framework of half-duplex amplify-and-forward protocol.
- Packet re-transmissions follows the Chase-type ARQ mechanism.
- Each Packet transmission k within a maximum of K ARQ rounds spans two consecutive time slots (TS)s.

Brief Description of the Concept

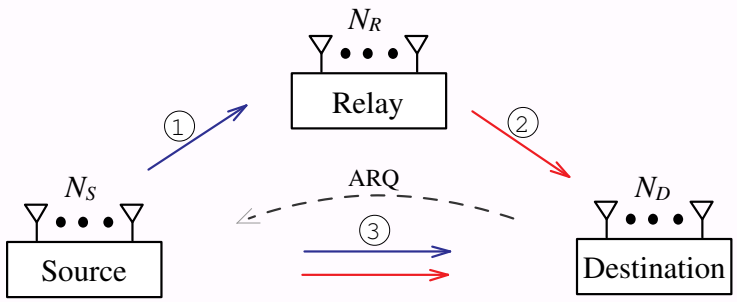

Fig. 1: Relay ARQ System Model

- Channel 1, channel 2, and channel 3 are regarded at kth transmission as a frequency selective fading MIMO channels having L_{SR}, L_{RD}, and L_{SD} independent paths, respectively.
- Each path is characterized by its quasi-static flat fading MIMO channel matrix $\mathbf{H}_l^{AB(k)} \in \mathbb{C}^{N_A \times N_B}$ for $l \in \{0, \ldots, L_{AB} - 1\}$ where $A \in \{S, R\}$ and $B \in \{R, D\}$.
- Relaying works under the framework of half-duplex amplify-and-forward protocol.
- Packet re-transmissions follows the Chase-type ARQ mechanism.
- Each Packet transmission k within a maximum of K ARQ rounds spans two consecutive time slots (TS)s.

Brief Description of the Concept

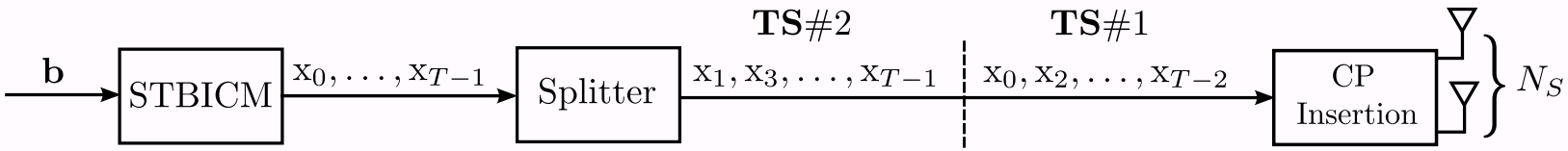

Fig. 2: Source node transmitter scheme.

Splitting Rule

- Upon the 1^{st} transmission, node S generates according to an STBICM encoder the symbol packet

$$\mathbf{x} \triangleq [\mathrm{x}_0, \ldots, \mathrm{x}_{T-1}] \in \mathbb{C}^{N_S \times T}. \tag{1}$$

- The symbol vectors $\mathrm{x}_{t'} \in \mathcal{X}^{N_S \times 1}$ for $t' = 0, \cdots, T-1$ are chosen to have equally powered entries, hence satisfying $\mathrm{E}[\mathrm{x}_{t'} \mathrm{x}_{t''}^{\mathrm{H}}] = \delta_{t',t''} \mathbf{I}_{N_S}$.
- It is then splitted into two equally sized $N_S \times \frac{T}{2}$ sub-packets $\mathbf{z}_1$ and $\mathbf{z}_2$ constructed as

$$\begin{cases} \mathrm{z}_{1,t} = \mathrm{x}_{2t} & , \quad 0 \leq t \leq \frac{T}{2} - 1 \\ \mathrm{z}_{2,t} = \mathrm{x}_{2t+1} & , \quad 0 \leq t \leq \frac{T}{2} - 1 \end{cases}. \tag{2}$$

Brief Description of the Concept

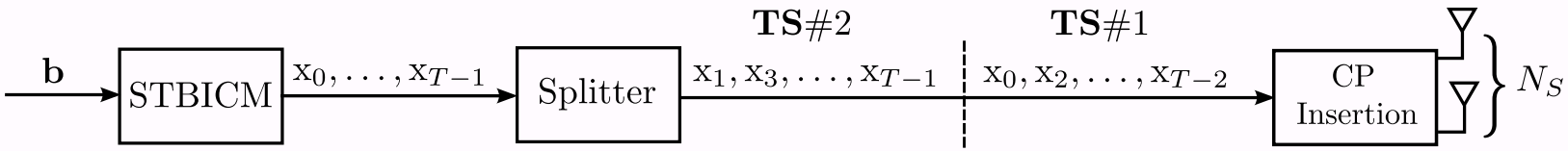

Fig. 2: Source node transmitter scheme.

Splitting Rule

- Upon the 1^{st} transmission, node S generates according to an STBICM encoder the symbol packet

$$\mathbf{x} \triangleq [x_0, \ldots, x_{T-1}] \in \mathbb{C}^{N_S \times T}. \tag{1}$$

- The symbol vectors $x_{t'} \in \mathcal{X}^{N_S \times 1}$ for $t' = 0, \cdots, T-1$ are chosen to have equally powered entries, hence satisfying $\mathrm{E}[x_{t'} x_{t''}^{\mathrm{H}}] = \delta_{t',t''} \mathbf{I}_{N_S}$.
- It is then splitted into two equally sized $N_S \times \frac{T}{2}$ sub-packets $\mathbf{z}_1$ and $\mathbf{z}_2$ constructed as

$$\begin{cases} z_{1,t} = x_{2t} & , \quad 0 \leq t \leq \frac{T}{2} - 1 \\ z_{2,t} = x_{2t+1} & , \quad 0 \leq t \leq \frac{T}{2} - 1 \end{cases}. \tag{2}$$

Brief Description of the Concept

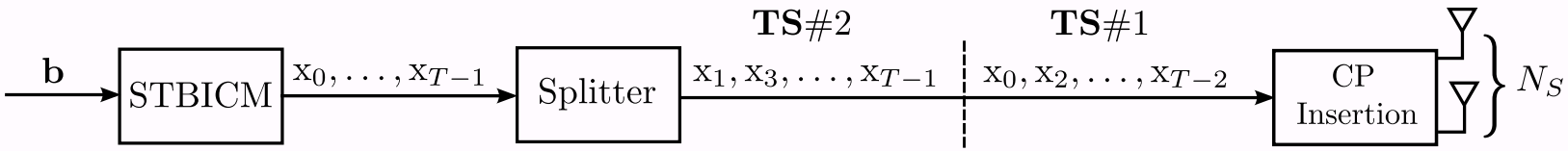

Fig. 2: Source node transmitter scheme.

Splitting Rule

- Upon the 1^{st} transmission, node S generates according to an STBICM encoder the symbol packet

$$\mathbf{x} \triangleq [x_0, \ldots, x_{T-1}] \in \mathbb{C}^{N_S \times T}. \tag{1}$$

- The symbol vectors $x_{t'} \in \mathcal{X}^{N_S \times 1}$ for $t' = 0, \cdots, T-1$ are chosen to have equally powered entries, hence satisfying $\mathrm{E}[x_{t'} x_{t''}^{\mathrm{H}}] = \delta_{t',t''} \mathbf{I}_{N_S}$.
- It is then splitted into two equally sized $N_S \times \frac{T}{2}$ sub-packets $\mathbf{z}_1$ and $\mathbf{z}_2$ constructed as

$$\begin{cases} z_{1,t} = x_{2t} & , \quad 0 \leq t \leq \frac{T}{2} - 1 \\ z_{2,t} = x_{2t+1} & , \quad 0 \leq t \leq \frac{T}{2} - 1 \end{cases}. \tag{2}$$

Relay ARQ Protocol

	Trans. (k)	
	1st TS	2nd TS
(S)	$\mathbf{z}_1$	$\mathbf{z}_2$
(R)	$\mathbf{y}_R^{(k)}$	$\tilde{\mathbf{y}}_R^{(k)}$
(D)	$\mathbf{y}_D^{1,(k)}$	$\mathbf{y}_D^{2,(k)}$

(a)

	Trans. (k odd)		Trans. (k even)	
	1st TS	2nd TS	1st TS	2nd TS
(S)	$\mathbf{z}_1$	$\mathbf{z}_2$	$\mathbf{z}_2$	$\mathbf{z}_1$
(R)	$\mathbf{y}_R^{(k)}$	$\tilde{\mathbf{y}}_R^{(k)}$	$\mathbf{y}_R^{(k)}$	$\tilde{\mathbf{y}}_R^{(k)}$
(D)	$\mathbf{y}_D^{1,(k)}$	$\mathbf{y}_D^{2,(k)}$	$\mathbf{y}_D^{1,(k)}$	$\mathbf{y}_D^{2,(k)}$

(b)

Transmission Period Reception Period

Fig. 3: Relay ARQ Protocol (a), Relay ARQ with Slot-Mapping Reversal (b) for $k = 1, \ldots, K$.

Sub-Packets Slot Mapping is Fixed Fig. 3(a)

- $\mathbf{z}_1$ followed by $\mathbf{z}_2$ during the first and the second TS, respectively, for all the ARQ rounds.

Relay ARQ with Slot Mapping Reversal

	Trans. (k)	
	1st TS	2nd TS
(S)	$\mathbf{z}_1$	$\mathbf{z}_2$
(R)	$\mathbf{y}_{\mathrm{R}}^{(k)}$	$\widetilde{\mathbf{y}}_{\mathrm{R}}^{(k)}$
(D)	$\mathbf{y}_{\mathrm{D}}^{1,(k)}$	$\mathbf{y}_{\mathrm{D}}^{2,(k)}$

(a)

	Trans. (k odd)		Trans. (k even)	
	1st TS	2nd TS	1st TS	2nd TS
(S)	$\mathbf{z}_1$	$\mathbf{z}_2$	$\mathbf{z}_2$	$\mathbf{z}_1$
(R)	$\mathbf{y}_{\mathrm{R}}^{(k)}$	$\widetilde{\mathbf{y}}_{\mathrm{R}}^{(k)}$	$\mathbf{y}_{\mathrm{R}}^{(k)}$	$\widetilde{\mathbf{y}}_{\mathrm{R}}^{(k)}$
(D)	$\mathbf{y}_{\mathrm{D}}^{1,(k)}$	$\mathbf{y}_{\mathrm{D}}^{2,(k)}$	$\mathbf{y}_{\mathrm{D}}^{1,(k)}$	$\mathbf{y}_{\mathrm{D}}^{2,(k)}$

(b)

Transmission Period Reception Period

Fig. 3: Relay ARQ Protocol (a), Relay ARQ with Slot-Mapping Reversal (b) for $k = 1, \ldots, K$.

Sub-Packets Slot Mapping is Reversed Fig. 3(b)

- Depending on the transmission index parity, sub-packets $\mathbf{z}_1$ and $\mathbf{z}_2$ are mapped onto either the first or the second time slot.

Sub-Packets ARQ Transmission Model (I)

During the 1^{st} TS of ARQ round k:

$$\mathbf{y}_{R,t}^{(k)} = \sqrt{\mathrm{E}_{SR}} \sum_{l=0}^{L_{SR}-1} \mathbf{H}_{l}^{SR^{(k)}} \mathbf{z}_{1,(t-l)\bmod \frac{T}{2}} + \mathbf{n}_{R,t}^{(k)} \quad (3)$$

$$\mathbf{y}_{D,t}^{1,(k)} = \sqrt{\mathrm{E}_{SD}} \sum_{l=0}^{L_{SD}-1} \mathbf{H}_{1,l}^{SD^{(k)}} \mathbf{z}_{1,(t-l)\bmod \frac{T}{2}} + \mathbf{n}_{D,t}^{1,(k)} \quad (4)$$

- E_{SR} and E_{SD} are the energies capturing the effects of path loss and shadowing in channel 1 and 3, respectively.
- $\mathbf{n}_{B,t}^{(k)} \sim \mathcal{N}(\mathbf{0}_{N_B \times 1}, N_0 \mathbf{I}_{N_B})$ for $B \in \{R, D\}$.
- A cyclic prefix (CP) portion of length $L_{cp} = \max\{L_{SD}, L_{SR}, L_{RD}\}$ is appended to $\mathbf{z}_1$ and $\mathbf{z}_2$ upon their transmission.

AF function at the Relay node:

$$\begin{cases} \widetilde{\mathbf{y}}_{R,t}^{(k)} = \gamma \mathbf{y}_{R,t}^{(k)}, \quad t = 0, ..., \frac{T}{2} - 1 \\ \gamma = 1/\sqrt{N_S \mathrm{E}_{SR} + N_0} \end{cases} \quad (5)$$

Sub-Packets ARQ Transmission Model (II)

During the 2^{nd} TS of ARQ round k:

$$\mathbf{y}_{D,t}^{2,(k)} = \sum_{l=0}^{L_{max}-1} \widetilde{\mathbf{H}}_{l}^{(k)} \mathbf{z}_{(t-l) \bmod \frac{T}{2}} + \widetilde{\mathbf{n}}_{D,t}^{2,(k)} \tag{6}$$

where

$$\begin{cases} \mathbf{z}_t & \triangleq \begin{bmatrix} \mathbf{z}_{1,t} \\ \mathbf{z}_{2,t} \end{bmatrix} \in \mathcal{X}^{2N_S}, \\ L_{max} & \triangleq \max(L_{SD}, L_{SRD}), \text{ and } L_{SRD} = L_{SR} + L_{RD} - 1, \end{cases} \tag{7}$$

$$\widetilde{\mathbf{H}}_{l}^{(k)} = \left[\gamma \sqrt{\mathrm{E}_{SR}\mathrm{E}_{RD}} \underline{\mathbf{H}}_{l}^{SRD^{(k)}} \quad \sqrt{\mathrm{E}_{SD}} \underline{\mathbf{H}}_{2,l}^{SD^{(k)}} \right],$$

$$\widetilde{\mathbf{n}}_{D,t}^{2,(k)} = \gamma \sqrt{\mathrm{E}_{RD}} \sum_{l=0}^{L_{RD}-1} \mathbf{H}_{l}^{RD^{(k)}} \mathbf{n}_{R,(t-l) \bmod \frac{T}{2}}^{(k)} + \mathbf{n}_{D,t}^{2,(k)}. \tag{8}$$

Sub-Packets ARQ Transmission Model (III)

At the end of the second slot node D builds up (jointly) the augmented size signal vector

$$\mathbf{y}_{D,t}^{equ(k)} \left\{ \begin{bmatrix} \mathbf{y}_{D,t}^{1,(k)} \\ \widetilde{\mathbf{y}}_{D,t}^{2,(k)} \end{bmatrix} \right. = \sum_{l=0}^{L_{max}-1} \mathbf{H}_l^{equ(k)} \mathbf{z}_{(t-l) \bmod \frac{T}{2}} + \mathbf{n}_{D,t}^{equ(k)}, \tag{9}$$

in which the k-parity $2N_D \times 2N_S$ equivalent MIMO channel matrix $\mathbf{H}_l^{equ(k)}$ has been carefully introduced with the following form

$$\begin{cases} \mathbf{H}_l^{equ(k)} = \begin{bmatrix} \mathbf{A} & \mathbf{0}_{N_D \times N_S} \\ \mathbf{B} & \mathbf{C} \end{bmatrix}, & k \text{ odd} \\ \mathbf{H}_l^{equ(k)} = \begin{bmatrix} \mathbf{0}_{N_D \times N_S} & \mathbf{A} \\ \mathbf{C} & \mathbf{B} \end{bmatrix}, & k \text{ even} \end{cases} \tag{10}$$

where,

$$\mathbf{A} = \sqrt{\mathrm{E}_{SD}} \underline{\mathbf{H}}_{1,l}^{SD^{(k)}}, \tag{11}$$

$$\mathbf{B} = \gamma \sqrt{\mathrm{E}_{SR}\mathrm{E}_{RD}} \mathrm{L}^{-1} \underline{\mathbf{H}}_{l}^{SRD^{(k)}}, \tag{12}$$

$$\mathbf{C} = \sqrt{\mathrm{E}_{SD}} \mathrm{L}^{-1} \underline{\mathbf{H}}_{2,l}^{SD^{(k)}}. \tag{13}$$

Sub-Packets ARQ Transmission Model (III)

In a joint manner signal vector $\mathbf{y}_{D,t}^{equ}{}^{(k)}$ is grouped with all the previously received signals $\mathbf{y}_{D,t}^{equ}{}^{(k-1)}, \cdots, \mathbf{y}_{D,t}^{equ}{}^{(1)}$ to decode the data packet.

K ARQ rounds Transmission Model

This leads to the $2N_D k \times 2N_s$ block transmission model given by

$$\underbrace{\begin{bmatrix} \mathbf{y}_{D,t}^{equ}{}^{(1)} \\ \vdots \\ \mathbf{y}_{D,t}^{equ}{}^{(k)} \end{bmatrix}}_{\mathbf{y}_{D,t}^{equ,k}} = \sum_{l=0}^{L_{max}-1} \underbrace{\begin{bmatrix} \mathbf{H}_l^{equ}{}^{(1)} \\ \vdots \\ \mathbf{H}_l^{equ}{}^{(k)} \end{bmatrix}}_{\mathbf{H}_l^{equ,k}} \mathbf{z}_{(t-l)\bmod \frac{T}{2}} + \underbrace{\begin{bmatrix} \mathbf{n}_{D,t}^{equ}{}^{(1)} \\ \vdots \\ \mathbf{n}_{D,t}^{equ}{}^{(k)} \end{bmatrix}}_{\mathbf{n}_{D,t}^{equ,k}}. \quad (14)$$

Outage Probability

Definition (Pertaining to K=1)

The outage probability at a given signal-to-noise ratio (SNR) ρ, denoted by P_{out}, refers to the probability half of the information rate $\mathcal{I}$ (the factor $\frac{1}{2}$ comes from the fact that one channel use of the equivalent received signal model (9) corresponds to two temporal channel uses), between transmitted block $\underline{\mathbf{z}}$ and received block $\underline{\mathbf{y}}_{\mathrm{D}}^{equ,1}$, is below a target rate $\mathcal{R}$,

$$P_{out}\left(\rho,\mathcal{R}\right)=\Pr\left\{\frac{1}{2}\mathcal{I}\left(\underline{\mathbf{z}};\underline{\mathbf{y}}_{\mathrm{D}}^{equ,1}\left|\left\{\mathbf{H}_{l}^{equ,1}\right\},\rho\right.\right)<\mathcal{R}\right\} \tag{15}$$

where

$$\underline{\mathbf{z}}=\begin{bmatrix}\mathbf{z}_{1}\\ \vdots\\ \mathbf{z}_{\frac{T}{2}}\end{bmatrix},\ \text{and}\ \ \underline{\mathbf{y}}_{\mathrm{D}}^{equ,1}=\begin{bmatrix}\mathbf{y}_{\mathrm{D},1}^{equ,1}\\ \vdots\\ \mathbf{y}_{\mathrm{D},\frac{T}{2}-1}^{equ,1}\end{bmatrix}.$$

Outage Probability

Generalization

To extend the previous formula on our ARQ relay system, we use the renewal theory as well as the observation that allows us to view the presented Chase-type ARQ mechanism, with a maximum number of rounds K, as a repetition coding scheme over K parallel sub-virtual channels. Accordingly, given the equivalent MIMO-ARQ channel model (14), (15) can be re-written as

$$P_{out}\left(\rho,\mathcal{R}\right)=\Pr\left\{\frac{1}{2K}\mathcal{I}\left(\underline{\mathrm{z}};\underline{\mathbf{y}}_{\mathrm{D}}^{equ,K}\left|\left\{\mathbf{H}_{l}^{equ,K}\right\},\rho\right.\right)<\mathcal{R},\overline{\mathcal{A}}_{1},...,\overline{\mathcal{A}}_{K-1}\right\},$$

where $\overline{\mathcal{A}}_{k}$ represents the event that a NACK feedback is sent back to the source node S at round $k=1,...,K-1$.

Average Throughput

The average throughput formula corresponding to the transmission over the equivalent Relay ARQ MIMO channel is given by

$$\eta = \frac{\mathrm{E}\left[\mathrm{R}\right]}{\mathrm{E}\left[\nu\right]}. \tag{16}$$

- R is a discrete random variable equals either to $\mathcal{R}$ when successful packet decoding is detected within the K rounds or 0 otherwise.
- In an outage sense, these two values are taken with probabilities $1 - P_{\overline{out}}\left(\rho, \mathcal{R}\right)$ and $P_{\overline{out}}\left(\rho, \mathcal{R}\right)$, respectively.
- ν is a RV counting the number of rounds consumed to transmit one packet.

Thus, the **average throughput** (16) can be re-expressed as

$$\eta = \mathcal{R}_{\nu}\left(1 - P_{\overline{out}}\left(\rho, \mathcal{R}\right)\right) \tag{17}$$

where $\mathcal{R}_{\nu} = \mathcal{R}/\mathrm{E}\left[\nu\right]$.

Scenario 1

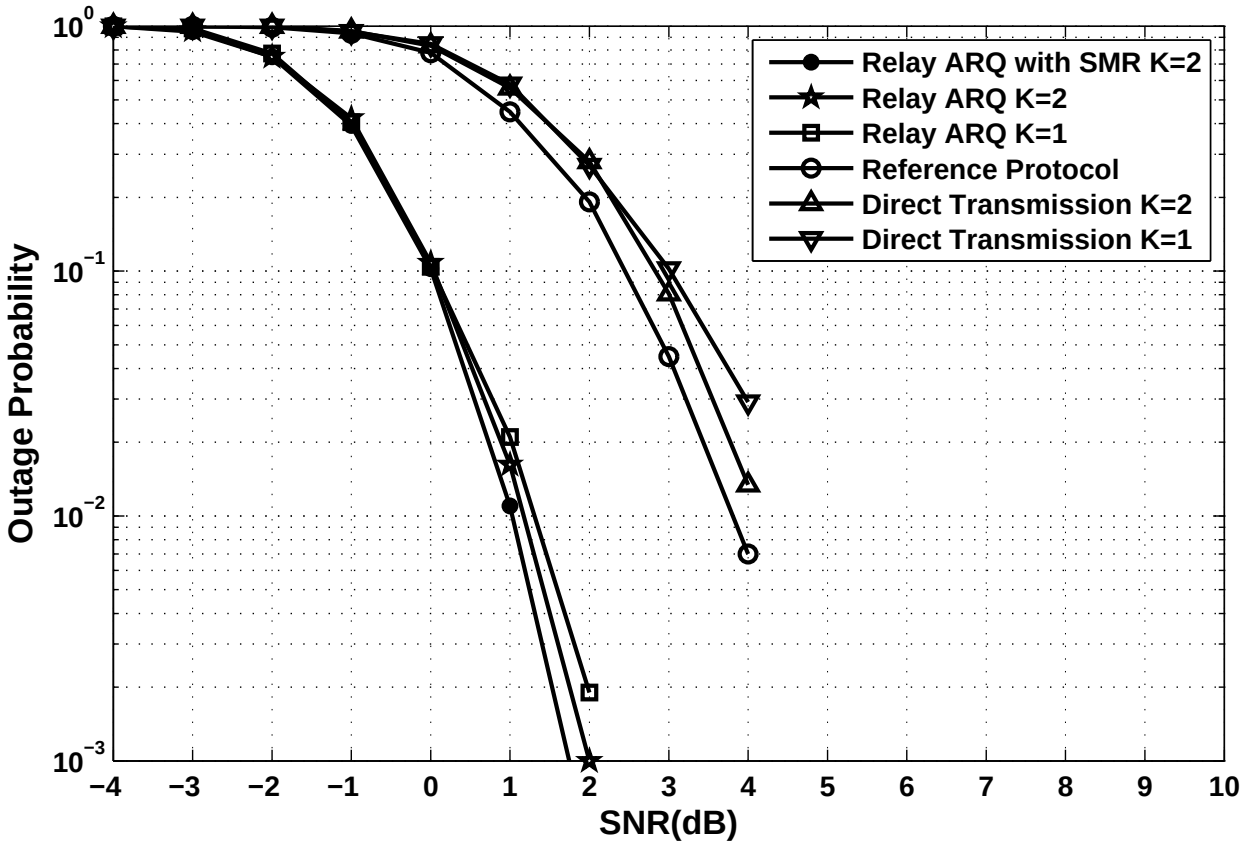

Fig. 4: Outage probability versus SNR for $l_{SR} = 0.3$, $N_S = N_R = N_D = 2$, $L_{SR} = L_{RD} = L_{SD} = 3$, and $\kappa = 3$.

Scenario 2

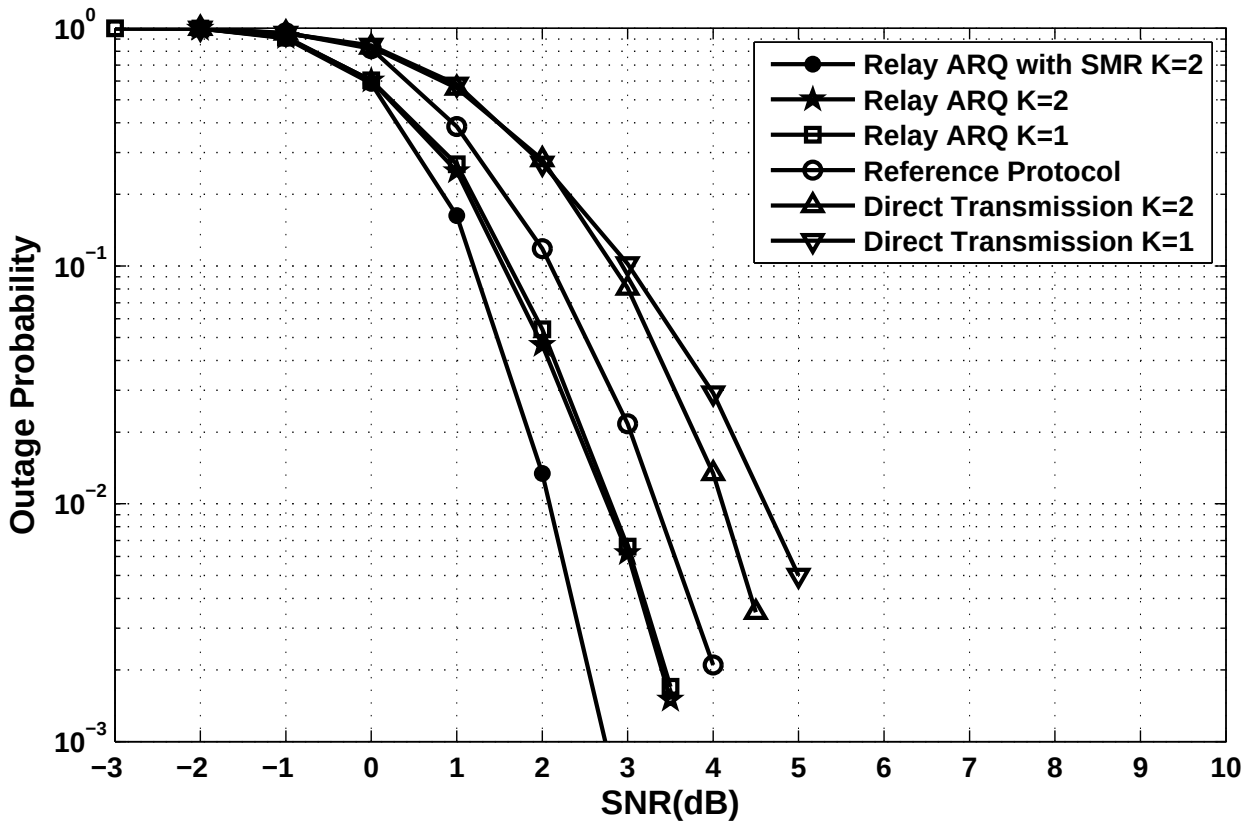

Fig. 5: Outage probability versus SNR for $l_{SR} = 0.7$, $N_S = N_R = N_D = 2$, $L_{SR} = L_{RD} = L_{SD} = 3$, and $\kappa = 3$.

Scenario 1

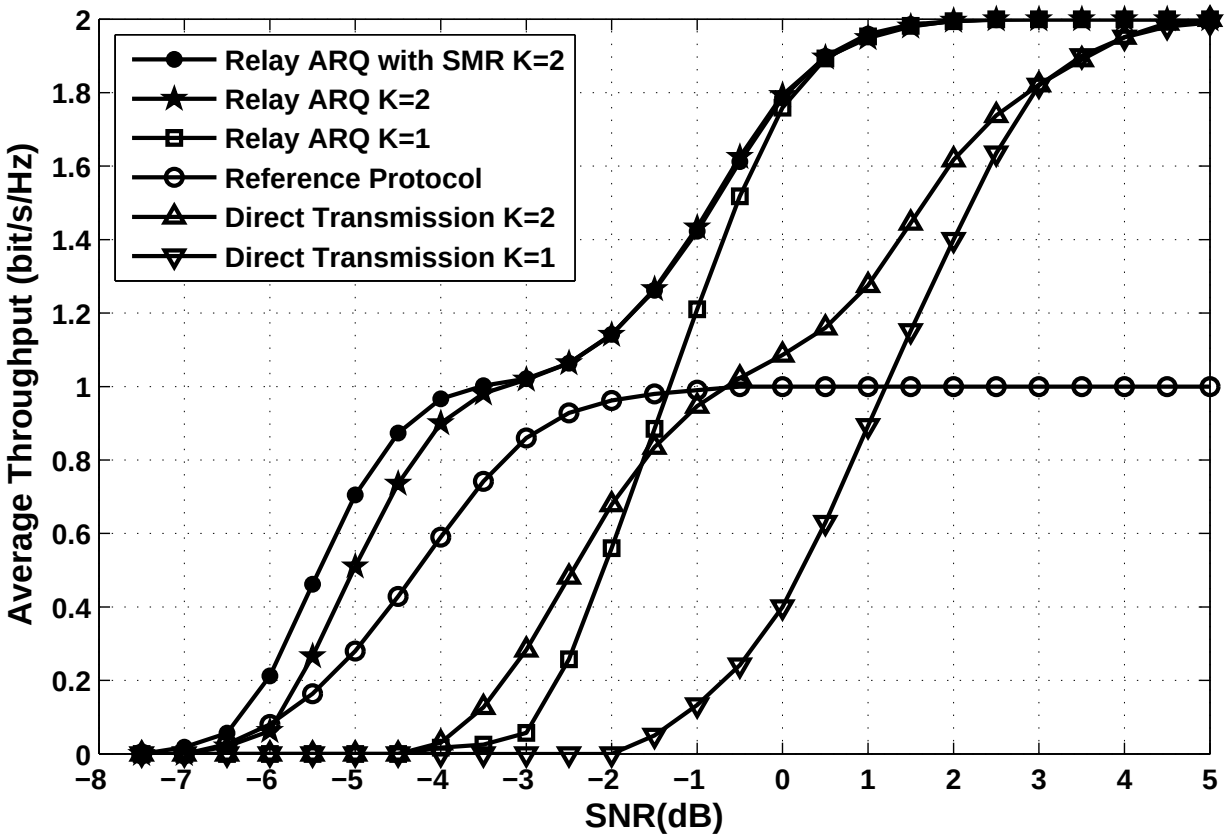

Fig. 6: Average throughput versus SNR for $l_{SR} = 0.3$, $N_S = N_R = N_D = 2$, $L_{SR} = L_{RD} = L_{SD} = 3$, and $\kappa = 3$.

Scenario 2

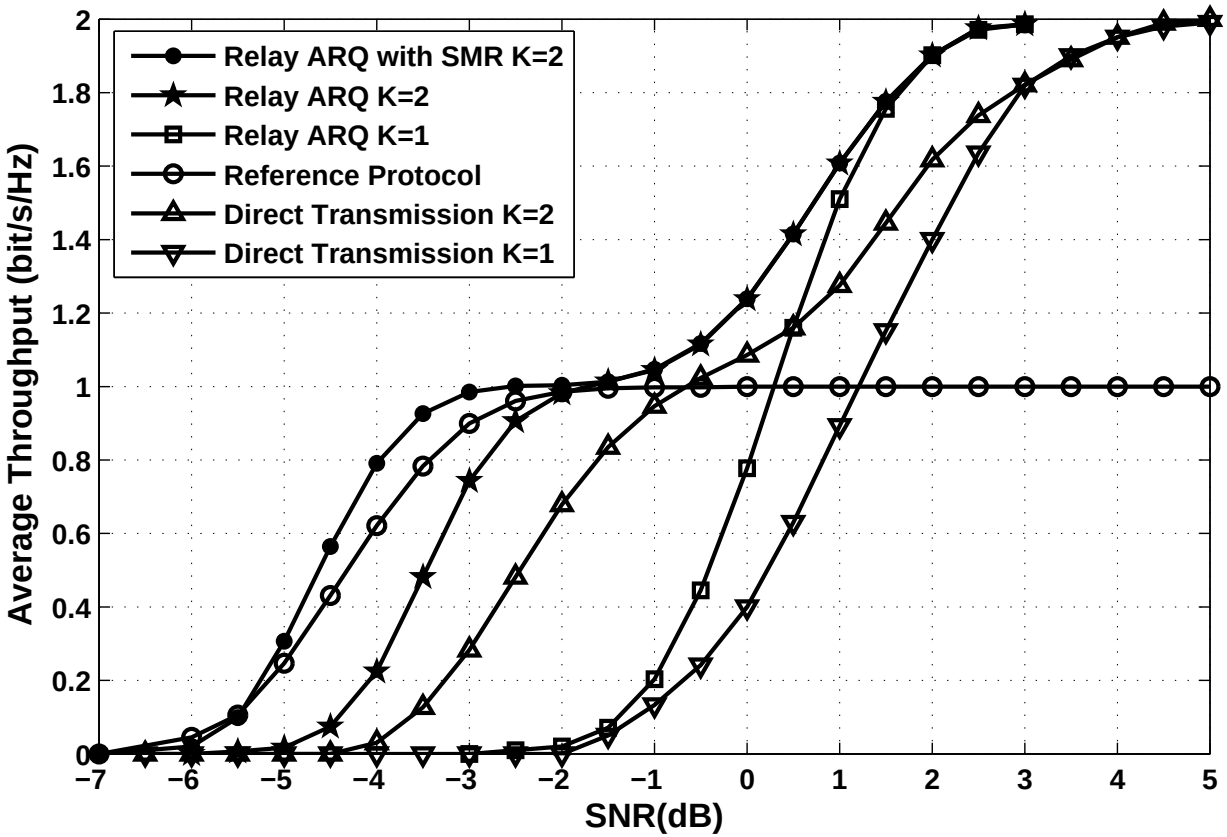

Fig. 7: Average throughput versus SNR for $l_{SR} = 0.7$, $N_S = N_R = N_D = 2$, $L_{SR} = L_{RD} = L_{SD} = 3$, and $\kappa = 3$.

Conclusion

- **New throughput-efficient relay ARQ techniques are investigated.**
- The half-duplex constraint has been turned from a disadvantage causing a multiplexing gain loss to an advantage providing significant improvement in average throughput & outage probability performance.
- Relay ARQ with slot mapping reversal provides considerable gain in terms of both outage prob. & average throughput over the entire SNR region.

Conclusion

- **New throughput-efficient relay ARQ techniques are investigated.**
- **The half-duplex constraint has been turned from a disadvantage causing a multiplexing gain loss to an advantage providing significant improvement in average throughput & outage probability performance.**
- **Relay ARQ with slot mapping reversal provides considerable gain in terms of both outage prob. & average throughput over the entire SNR region.**

Conclusion

- **New throughput-efficient relay ARQ techniques are investigated.**
- **The half-duplex constraint has been turned from a disadvantage causing a multiplexing gain loss to an advantage providing significant improvement in average throughput & outage probability performance.**
- **Relay ARQ with slot mapping reversal provides considerable gain in terms of both outage prob. & average throughput over the entire SNR region.**

Perspectives

- **It is recommended to design practical turbo receivers that can approach the previous theoretical limits.**
- Analytical results of the outage probability and average throughput instead of Monte-Carlo based simulations should be investigated.
- Extension of the proposed techniques to a multi-user environment where several relays are deployed.

Perspectives

- **It is recommended to design practical turbo receivers that can approach the previous theoretical limits.**
- **Analytical results of the outage probability and average throughput instead of Monte-Carlo based simulations should be investigated.**
- **Extension of the proposed techniques to a multi-user environment where several relays are deployed.**

Perspectives

- **It is recommended to design practical turbo receivers that can approach the previous theoretical limits.**
- **Analytical results of the outage probability and average throughput instead of Monte-Carlo based simulations should be investigated.**
- **Extension of the proposed techniques to a multi-user environment where several relays are deployed.**

Related Works

- Houda Chafnaji, Tarik Ait-Idir, Halim Yanikomeroglu, and Samir Saoudi, "Analysis of Packet Combining for Single Carrier Multi-Relay Broadband Systems," in Proc., IEEE International Workshop on Signal Processing Advances in Wireless Communications, SPAWC 2010, Marrakech, Morocco, Jun. 2010.
- Houda Chafnaji, Halim Yanikomeroglu, Tarik Ait-Idir, and Samir Saoudi, "Turbo Packet Combining Techniques for Multi-Relay-Assisted Systems over Multi-Antenna Broadband Channels," in Proc., ACM International Wireless Communications and Mobile Computing Conference, IWCMC 2010, Caen, France, Jun. 2010.
- Tarik Ait-Idir, and Samir Saoudi, "Turbo Packet Combining Strategies for the MIMO-ISI ARQ Channel," IEEE Transactions on Communications, vol. 57, no. 12, pp. 3782-3793, Dec. 2009.
- Houda Chafnaji, Tarik Ait-Idir, Halim Yanikomeroglu, and Samir Saoudi, "Joint Turbo Equalization for Relaying Schemes over Frequency-Selective Fading Channels," in Proc., ACM International Wireless Communications and Mobile Computing Conference, IWCMC 2009, Leipzig, Germany, Jun. 2009.